

Original Research Paper

Cohesion Analysis of Rubber Stand Ages Using Object-Based Image Analysis and Spatial Autocorrelation

¹Jiradech Majandang, ¹Suepsai Prasansat, ²Patiwat Littidej, ²Phusit Khamphilung, ¹Nanthaporn Usaard, ³Benjamabhorn Pumhirunroj and ⁴Donald Slack

¹Department of Geography, Faculty of Humanities and Social Sciences, Maharakham University, Maharakham, Thailand

²Department of Geoinformatics, Research Unit of Geoinformatics for Spatial Management, Faculty of Informatics, Maharakham University, Maharakham, Thailand

³Department of Animal Science, Faculty of Agricultural Technology, Sakon Nakhon Rajabhat University, Sakon Nakhon, Thailand

⁴Department of Civil and Architectural Engineering and Mechanics, the University of Arizona, Arizona, USA

Article history

Received: 27-04-2024

Revised: 08-06-2024

Accepted: 09-08-2024

Corresponding Author:

Patiwat Littidej
Department of Geoinformatics,
Research Unit of
Geoinformatics for Spatial
Management, Faculty of
Informatics, Maharakham
University, Maharakham,
Thailand
Email: patiwat.1@msu.ac.th

Abstract: Latex and rubber wood are crucial raw materials used in various industries and play a significant role in the economies of many countries, particularly in tropical regions. Mapping the areas where these materials are planted and classifying the age of rubber stands is important for managing growth assessment, yield assessment, and estimating the number of mature rubber trees that will be harvested. In this study, we conducted a visual interpretation of high-resolution satellite imagery from Google Earth in Mueang Loei District, Loei Province, Thailand. We discovered a total of 443.78 square kilometers of rubber plantations on the west side of the research area. The rubber stands were categorized into four age groups: Under seven years old, seven to fifteen years old, fifteen to twenty-five years old, and over twenty-five years old. To analyze the age classification accuracy, we employed Object-Based Image Analysis (OBIA) using the Hierarchical classification technique with Sentinel-2A images. We compared the results with the overall accuracy and Kappa coefficient of agreement between the ground-truth data and Google Earth satellite imagery. As the planting zones were not ordered within the research area, all four age groups were combined inside the rubber plantation area. The Kappa coefficient is 68.55 and the overall accuracy is 77.23%. This can be attributed to the fact that rubber farming is still in its early stages in the region. The area occupied by rubber plantations in the 15-25-year-old and 7-15-year-old age groups is 99.40 (22.40%) and 169.23 (38.13%) square kilometers, respectively. The area occupied by rubber plantations in less than 7 years is 96.85 (21.82%) square kilometers. The results are reliable as they validate the spatial relevance of each age group's rubber plantation size to the outcomes of the image analysis with clustered spatial correlation. The findings of this study demonstrate that OBIA can be used to categorize rubber age ranges, particularly for middle-aged (7-15 years old and 15-25 years old) and mature (>25 years old) rubber with similar canopy features. The information obtained from this study can be utilized to analyze the issue of declining rubber prices due to the surplus production from numerous rubber plantations, which may lead some farmers to convert their land to other cash crops.

Keywords: Rubber Plantation, Object-Based Image Analysis (OBIA), Remote Sensing, Loei Province of Thailand

Introduction

Natural rubber is a crucial commodity for the global economy (Lemes *et al.*, 2020). It is used as a raw material in more than 40,000 industrial and non-industrial products (Van Beilen and Poirier, 2007). Additionally, it is a renewable resource with exceptional properties such as flexibility, high elasticity, toughness, and low heat build-up during use (Longsen and Khaokong, 2020). In 2020, the production of natural rubber reached 14.84 million tons, with Thailand, Indonesia, Vietnam, and India being the major producing countries Food and Agriculture Organization of the United Nations (FAO), 2022). The rubber tree, scientifically known as *Hevea brasiliensis*, is responsible for producing over 99% of natural rubber (Prasongsansuk *et al.*, 2020; Vu *et al.*, 2020). According to FAO, the global area of rubber plantations was 12.80 million hectares in 2020, with approximately 9.67 million hectares (75.55%) located in Southeast Asia. This includes approximately 3.67 million hectares in Indonesia and 3.29 million hectares (27%) in Thailand.

Thailand is a leading global producer and exporter of natural rubber, making natural rubber a crucial plant for the country's economy (FAO, 2022). The cultivation of rubber trees began in 1899 in the Kantang District of Trang Province and since then, the planting area has steadily expanded. Rubber cultivation is widespread across 14 provinces in the southern region of Thailand, ranging from Chumphon Province to the provinces bordering Malaysia. This has led to the continuous growth and development of the rubber industry in the country (Littidej *et al.*, 2024). As of 2021, Thailand had approximately 3.91 million hectares of rubber plantations throughout the country, yielding a production quantity of 4.91 million tons Office of Agricultural Economics (OAE) 2022. Additionally, it has been discovered that rubber wood can serve as a valuable by-product when old rubber trees are cut down to be replaced. This is especially beneficial since rubber trees older than 25 years have low latex production, making it economically unfeasible to tap them for latex.

Therefore, rubber trees need to be cut down for replanting with new rubber trees or other crops (Lim *et al.*, 2003; Petsri *et al.*, 2013). Rubber wood can then be processed and used to make various products, including furniture, wood products, veneers, fuel, and paper pulp. The quality of the wood depends on its chemical and physical properties (Phoomchai *et al.*, 2015). In 2020, Thailand exported rubber wood from 2.34 million hectares, valued at 28.93 million baht (OAE, 2022). It is important to determine the age range of rubber trees to evaluate rubber latex yields (Chen *et al.*, 2018a) and assess the amount of rubber wood obtained from cutting down the trees (Azizan *et al.*, 2021). Additionally, determining the age range of rubber trees is crucial for studying the carbon cycle, including tracking biomass (Suratman *et al.*, 2004) and estimating carbon stocks (Blagodatsky *et al.*, 2016).

Remote sensing is a valuable tool for monitoring ecosystem changes, providing spatial and temporal information (Rogan *et al.*, 2003). In the context of rubber plantations, remote sensing has been applied in various ways, including mapping, change detection, stand age estimation, biomass, and carbon estimation, leaf area index estimation, and disease detection (Azizan *et al.*, 2021). Specifically, stand age estimation in rubber plantations using remote sensing can be approached through three practical methods: statistical models, image classification, and Land Use Land Cover Change (LULCC) detection (Chen *et al.*, 2018b).

Remote sensing indices can also be applied to study land use (Sarapirome, 2013) impacted by wildfires, air pollution analyzed using spatial models (Littidej and Aunphoklang, 2013; Littidej, 2017; Littidej *et al.*, 2013). and floods. Previous research by Prasertsri and Littidej (2020), Littidej *et al.* (2022); Littidej and Buasri (2019) has explored this. Additionally, RS is utilized in spatial epidemic studies (Pumhirunroj *et al.*, 2024), where image translation is an essential step in the modeling process (Pumhirunroj *et al.*, 2023). Image classification is a commonly used method for mapping vegetation distribution (Dibs and Hussain, 2018). Rubber plantations are typically categorized based on maturity or latex production level, as studied by Koedsin and Huete (2015); and Sayavong *et al.* (2019). To study forest stand age, medium spatial resolution imagery from sources like Landsat, Spot, or Sentinel-2 is crucial. These imagery sources are chosen due to their open-access policies and have been used in studies conducted by Chen *et al.* (2018b); Sayavong *et al.* (2019); Dibs *et al.* (2017); Yusof *et al.* (2021).

Pixel-based classification in remote sensing technologies involves grouping pixels using classification algorithms, without considering spatial association with neighboring pixels (Cleve *et al.*, 2008). However, this approach often leads to a "salt-and-pepper" effect in the classification results, as noted by Yu *et al.* (2006). To address this issue, object-based classification was developed (Zhang and Xie, 2013). This method segments an image into clusters of neighboring pixels that exhibit similar characteristics (objects) and then classifies these clusters based on the properties within the objects (Gibbes *et al.*, 2010; Cleve *et al.*, 2008; Kajisa *et al.*, 2009; Rawat and Kumar, 2015). Since 2000, Object-Based Image Analysis (OBIA) has been a continuously evolving field in image classification (Blaschke, 2010). It has gained wide acceptance and is extensively used for classifying high-resolution satellite data (Blaschke *et al.*, 2014; Myint *et al.*, 2011), as well as moderate-resolution satellite imagery (Kajisa *et al.*, 2009; Hamada *et al.*, 2013; Putklang *et al.*, 2019; Su and Zhang, 2021).

The main goal of this study is to use the object-based image analysis method to map the stand age of rubber plantations in Mueang Loei District, Loei Province, Northeast Thailand. For this purpose, Sentinel-2 satellite

imagery captured in December 2019 was utilized. The rubber plantations were classified into four age categories: 0-6 years, 7-15 years, 16-24 years, and over 25 years. The accuracy of the classification was verified by comparing it with field survey data and high spatial resolution satellite imagery from Google Earth. These methodologies have been employed to develop rubber management plans in the research area, which include growth monitoring, yield estimations, and estimating the volume of rubber wood produced by mature trees (over 25 years old).

Materials and Methods

Study Area

Mueang Loei district, located in Loei Province in northeastern Thailand, has geographical coordinates of 101° 43' 48" E to 17° 29' 6" N (Fig. 1). According to the Center (2023) of the Thai Meteorological Department (2023), the annual mean temperature in the area ranges from 21.1-32.5°C between 1991 and 2020. The average annual rainfall is between 900 and 1300 mm. The district experiences a cold season from October to February, characterized by the northeast monsoon bringing cold air from China. As a result, Loei province is known for its cold and dry weather. The hot season runs from February to May, followed by the rainy season from May to October. During the rainy season, the southwest monsoon draws moisture from the seas and oceans, leading to abundant rainfall. This combination of factors, including a low-pressure trough, makes Loei the province with the largest number of rubber-growing areas in the Northeast region, thanks to its favorable climate and topography. The Office of Agricultural Economics (OAE, 2022) reports that the area of rubber plantations has steadily increased since 2011, reaching 776.82 square kilometers in 2021, a growth of 714.16 km².

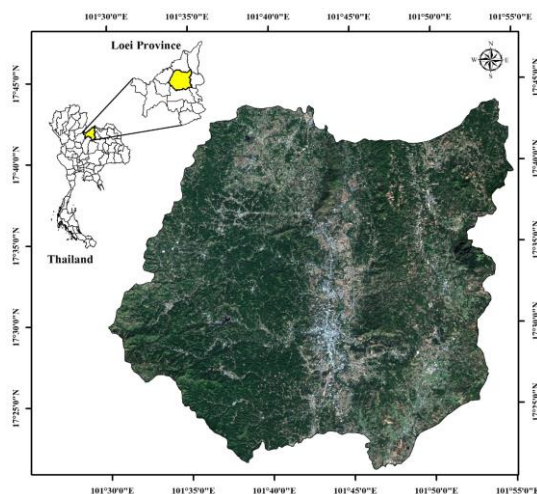


Fig. 1: Mueang Loei district, Loei Province in true color composite (bands 4, 3, and 2) of Sentinel-2 imagery

Data and Preprocessing

This study primarily utilized Sentinel-2 satellite data obtained from Sentinel-hub (<https://scihub.copernicus.eu>). The specific data used was recorded on December 3, 2019 (S2A_MSIL2A_20191203T034121_N0213_R061_T47QQ_V_20191203T141050.SAFE). Sentinel-2 imagery consists of a Multispectral Instrument (MSI) with 13 bands. The spatial resolution varies across the bands, with 10 m resolution for Bands 2, 3, 4, and 8, 20 m resolution for Bands 5, 6, 7, 8A, 11, 12 and 60 m resolution for Bands 1, 9 and 10. To enhance the image quality, a radiometric correction technique was applied. Specifically, the Haze Reduction Atmospheric effects method proposed by (Ahmad and Quegan, 2014) was used. This correction method helps to reduce atmospheric haze and dust, thereby improving the dynamic range and sharpening the image.

Ground Reference Data

The ground reference data was obtained from a field survey conducted in February 2020. In areas that were difficult to access due to lack of road crossing, photo interpretation was done using high spatial resolution satellite imagery from Google Earth. A total of 505 ground-truth data points were collected using a random stratified sampling strategy to select the checkpoint locations, as shown in Fig. (2). Field photographs were taken at four different stages of rubber tree growth: (a) rubber trees less than 7 years old, (b) rubber trees between 7 and 15 years old, (c) rubber trees between 15 and 25 years old and (d) rubber trees greater than 25 years old.



(a)



(b)



(c)



(d)

Fig. 2: Field photos taken on the February 2020; (a) Rubber tree less than 7 years old; (b) Rubber tree between 7 and 15 years old; (c) Rubber tree between 15 and 25 years old; (d) Rubber tree greater than 25 years old (photo credit: Suepsai Prasansat)

Mapping Rubber Plantations

The purpose of this study is to classify rubber plantations using high-resolution satellite imagery from Google Earth. By using the boundaries of rubber plantations as a reference, we aim to exclude other areas from the analysis of Sentinel-2 satellite imagery. This approach, known as Object-Based Image Analysis (OBIA), allows us to classify the age of rubber plantations without considering the reflection values of non-rubber areas. By implementing this method, we can reduce processing errors associated with different types of land use and improve the overall efficiency of rubber age classification. The classification is based on the visual appearance of the rubber plantations in the satellite images. Color tone, brightness, shape, size, pattern, texture, location and association, shadow, temporal change, and tone are all factors that were considered during the visual interpretation. To ensure accuracy, a field investigation was conducted to compare the rubber

plantation area depicted in the image with the actual site. Using Google Earth, the boundaries of the rubber plantation area were digitized on the screen at a scale of no greater than 1:4,000.

Image Segmentation

Multiresolution Segmentation is a method of image segmentation that groups similar or identical image points together based on parameters such as Band Weight, Scale, Color, Shape, Smoothness, and Compactness. It iteratively determines these parameters until the most appropriate segmentation for the image of a unified object is achieved. Although the scale parameter is known by its abstract values, it is necessary to evaluate the appropriate criterion. Therefore, prior to the classification, the optimal scale parameter was determined using ESP Tools (Drăguț *et al.*, 2010) in order to carry out the optimal scale parameters. The ESP Tools indicated a correlation between local variance and the rate of change among the image pixels, reflecting various scale parameters based on user-defined factors such as the initial scale parameter, shape, and compactness. The result obtained from this tool is presented as a relationship graph between the two variables mentioned above. Researchers have experimented with changing various parameters to obtain results that are best suited for the area. Lastly, the factors inputted into ESP TOOLS are as follows: StepSize_ScaleParameter = 1, ScaleParameter = 60, Loop = 100, shape = 0.4, and compactness = 0.8, as shown in Fig. (3). The results obtained using this tool indicate that the appropriate parameter scale for classifying rubber tree objects in the target image is 114. The satellite image was then subjected to multiresolution segmentation based on the results obtained from ESP TOOLS, with SP = 114, shape = 0.6, and compactness = 0.8. Additionally, a weight of 2 was assigned to the NIR band, while the other bands were given a weight of 1 to distinguish between vegetation and non-vegetation areas. The MRS result reveals that the selected satellite image contains a total of 14,675 image objects, as shown in Fig. (4).

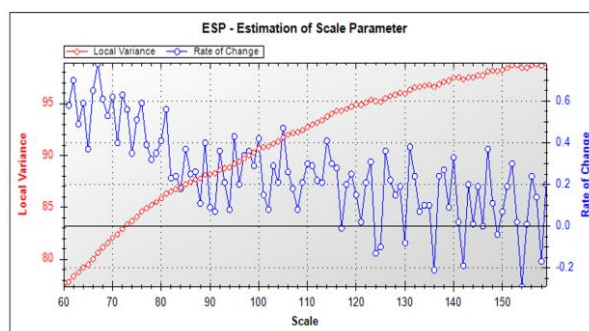


Fig. 3: The scale parameter estimation by using ESP TOOLS

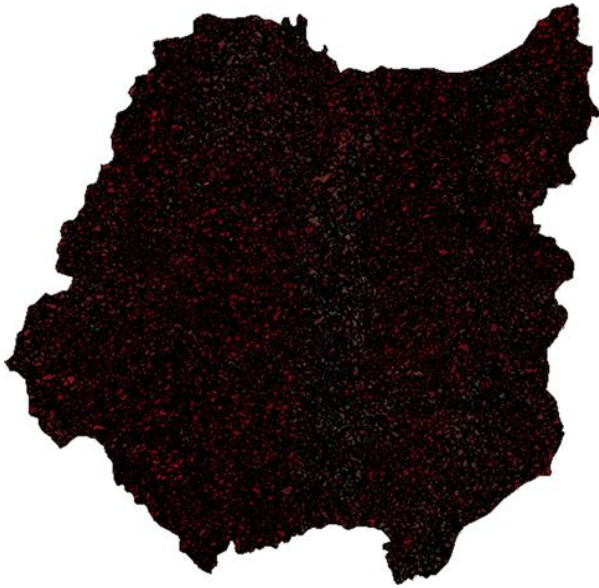


Fig. 4: Image objects derived from Multi-resolution segmentation algorithm

Table 1: Table type styles

Rubber stand ages	NDVI	GLCMs homogeneity	Brightness	Overall accuracy (%)
Less than 7 years old	0.639-0.718	0.1058-0.2431	229.988-242.917	83
7 and 15 years old	0.758-0.775	0.1058-0.2078	224.447-236.145	87
15 and 25 years old	0.761-0.782	0.0901-0.2156	211.517-232.451	74
Greater than 25 years old	0.768-0.806	0.1254-0.2627	209.670-225.678	66

Rubber Stand Ages Classification

The study utilized high spatial resolution satellite imagery from Google Earth in combination with a field survey to identify the training areas for each stage of rubber lifespan. A total of 25 training areas were designated for each age range, resulting in a grand total of 100 points across 4 different age ranges. The hierarchical classification of rubber stands ages involved grouping objects based on data obtained from the training areas, which were analyzed using multi-resolution segmentation and member functions derived from various data layers and parameters. The classification of rubber stand ages in this study is based on several data layers and key parameters. These include the Normalized Difference Vegetation Index (NDVI), Gray Level Co-occurrence Matrices (GLCMs), homogeneity and brightness. The classification ruleset was developed using a rule-based approach, utilizing class descriptions to distinguish between the lower and upper ranges of information associated with image objects. Table (1) for more details.

Accuracy Assessment

To assess the accuracy of rubber plantation, stand ages, an error matrix or confusion matrix is created. This matrix helps calculate various measures such as the producer's accuracy, the user's accuracy, overall accuracy, and the Kappa coefficient of agreement (Congalton and Green, 2008). The overall accuracy is determined by comparing the proportion of correctly classified points to all the sample points examined. In LULC assessments, the Kappa coefficient is commonly used to measure the true agreement between observed agreement and chance agreement in terms of accuracy. Equations (1-3) are used to calculate the Kappa coefficient:

$$Kappa = \frac{P_o - P_e}{1 - P_e} \quad (1)$$

where, P_o is the proportion of observed agreements and P_e is the proportion of agreements expedited by chance (Prasertsri and Littidej, 2020; Littidej *et al.*, 2022):

$$P_o = \sum_{i=1}^c P_{ij} \quad (2)$$

$$P_e = \sum_{i=1}^c P_i T_p T_j \quad (3)$$

where, P_{ij} is the i^{th} and the j^{th} cell of the contingency table, $p_i T$ is the sum of all cells in the i -th row, $p T_j$ is the sum of all cells in a j^{th} column and c is the count of the raster category.

Results and Discussion

Rubber Plantations Map Results

The rubber plantations in the study area cover a total of 443.78 square kilometers, which accounts for 34.72% of the district's total area. These plantations are spread throughout the entire area, but are particularly dense in the western part, as illustrated in Fig. (5).

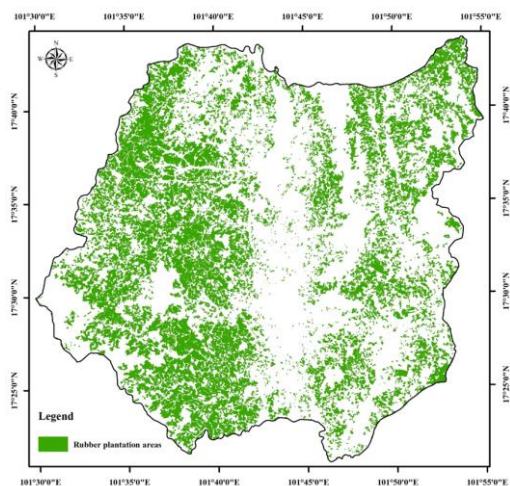


Fig. 5: Rubber plantations from visual classification with Google Earth imagery

Rubber Stand Ages Classification Results

The results of rubber age classification using Object-Oriented classification based on Sentinel-2 imagery are as follows: Rubber plantations less than 7 years old occupy an area of 96.85 square kilometers, those between 7 and 15 years old cover 169.23 square kilometers, those between 15 and 25 years old encompass 99.40 square kilometers and those older than 25 years occupy 78.30 square kilometers (Table 2). In Fig. (6), it can be observed that rubber trees between 15 and 25 years old as well as those older than 25 years are densely located in the western part of the study area. The area covered by rubber trees older than 25 years is the smallest due to this being the initial phase of rubber plantation experiments in the study area, which was encouraged by the government and influenced by high rubber prices as an incentive for farmers. On the other hand, the area covered by rubber trees between 15 and 25 years old and between 7 and 15 years old has been steadily increasing. However, the number of rubber trees less than 7 years old has been decreasing due to continuously falling rubber prices, leading some farmers to switch from rubber cultivation to other cash crops, particularly those that yield faster results such as field crops. Rubber areas can be classified based on different age ranges. However, due to a lack of planning to divide the planting age zone, there is a varied distribution within the area. As a result, each farmer cultivates their own rubber.

Table 2: Areas of rubber stand ages obtained from Sentinel-2 imagery

Rubber stand ages	Area (km ²)	Percent (%)
Less than 7 years old	96.85	21.82
7 and 15 years old	169.23	38.13
15 and 25 years old	99.40	22.40
Greater than 25 years old	78.30	17.64

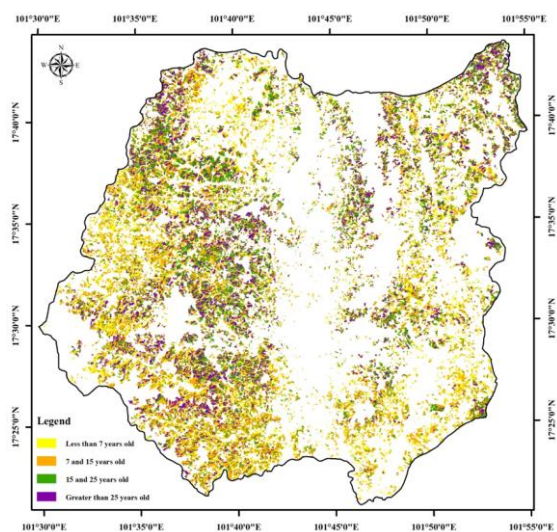


Fig. 6: Maps of rubber stand ages extracted from Sentinel-2 imagery

The assessment of the accuracy of rubber plantation stands ages revealed that the overall accuracy was 77.23%, with a Kappa coefficient of 68.55. The user's accuracies for rubber less than 7 years old, 7-15 years old, 15-25 years old, and greater than 25 years old were 82.72, 87.22, 74.19, and 65.71% respectively. The producer's accuracies for rubber in the age ranges of less than 7 years old, 7-15 years old, 15-25 years old, and greater than 25 years old were 94.37, 68.64, 78.41 and 77.53% respectively (Table 3). Based on the chart, the most suitable age range for rubber trees is less than 7 years. This study specifically focused on rubber trees within rubber-growing areas identified through Google Earth. This age range also contributes to the soil's reflectivity. When the rubber tree canopy reaches 15-25 years or older, it is considered fully grown. Therefore, the reflection values obtained from satellite photography can be compared. It is important to note that although Sentinel-2 satellite imagery has a higher resolution of 10 m compared to Landsat pictures (30 m, Pan-Sharpening 15 m), the resolutions are not equivalent. Additionally, the age range of the rubber trees directly affects the accuracy of the classification in relation to other studies. For example, the study by Sayavong *et al.* (2019) mapped rubber tree ages in Luangnamtha district (Northern Laos) using NDVI and LSWI from Landsat images and set the final value range at 11-12 years, <7 years old, 7-12 years old and >12 years old. The overall accuracies were 80 and 87%, with kappa coefficients of 0.67 and 0.79, respectively. Li and Fox (2012) used a MODIS satellite and the Mahala Nobis topicalities to classify rubber stand ages. They obtained a kappa coefficient of 0.76 by dividing the rubber plantations into two groups: <4 years old and ≥ 4 years old. Kou *et al.* (2015) integrated PLASAR and Landsat images in the classification of rubber stand ages. The overall accuracy was 85%, with a kappa coefficient of 0.78. They divided the ages into three groups: ≤ 5 years old, 6-10 years old, and ≥ 11 years old. Furthermore, the mountainous terrain of the study area, coupled with varying planting distances between rows in each plot, constitutes another factor that influences the classification of rubber plantation age (Sayavong *et al.*, 2019).

Table 3: The confusion matrix, producer's and user's accuracy of rubber stand ages classification result

Ages	Rubber stand				Total
	<7 years old	7-15 years old	15-25 years old	>25 years old	
<7 years old	67	9	2	3	81
7-15 years old	3	116	7	7	133
15-25 years old	1	37	138	10	186
>25 years old	0	7	29	69	105
Total	71	169	179	89	505
User's accuracy	82.72%	87.22%	78.41%	65.71%	
Producer's accuracy	94.37%	68.64%	77.53%		
overall accuracy = 77.23%					
Kappa coefficient = 68.55					

The classification of rubber plantations from Google Earth, using a geographically high-resolution satellite, helps to distinguish them from other types of land use. This method is effective in separating rubber plantations based on their stand ages. It is also important to note that there is no cost associated with determining the training area for classification or using this information to evaluate the accuracy of the classification, as demonstrated in previous studies (Li and Fox, 2012; Dong *et al.*, 2013; Kou *et al.*, 2015; Chen *et al.*, 2018a; Sayavong *et al.*, 2019).

OBIA simplifies and speeds up the classification of rubber tree ages, saving time and money on field surveys. Additionally, the collected data can be used to effectively manage planting areas and predict future yields. Rubber areas aged 7-15 years and those older than 15 years but younger than 25 years are particularly useful for forecasting future yields and arranging transportation for produce. Moreover, rubber areas older than 25 years help estimate the number of rubber trees that are ready for replanting.

Spatial autocorrelation analysis can support the analysis of rubber trees aged 0-7 years by confirming the interpretation of their age. Since farmers in the area practice monoculture, the study found that the results of rubber cohesion were consistent and clustered across all four age groups. This further supports the accurate identification of rubber trees using OBIA and satellite imagery translated from Sentinel-2A data. This effect is illustrated in Figs. 7(a-d).

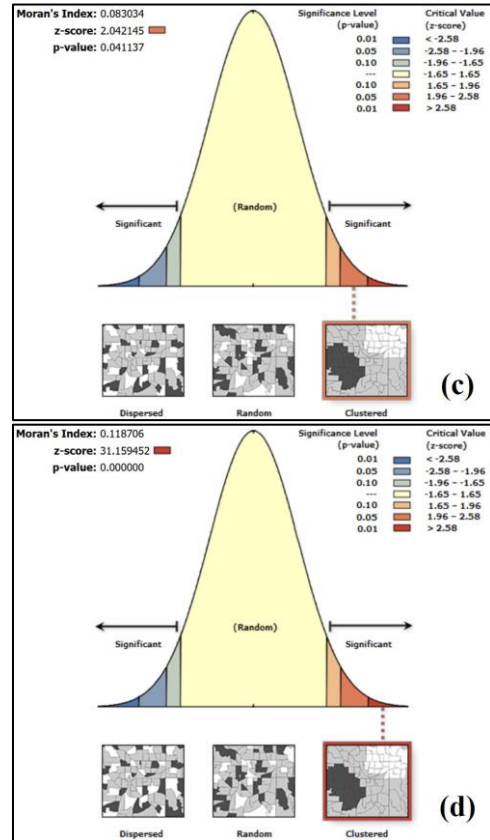
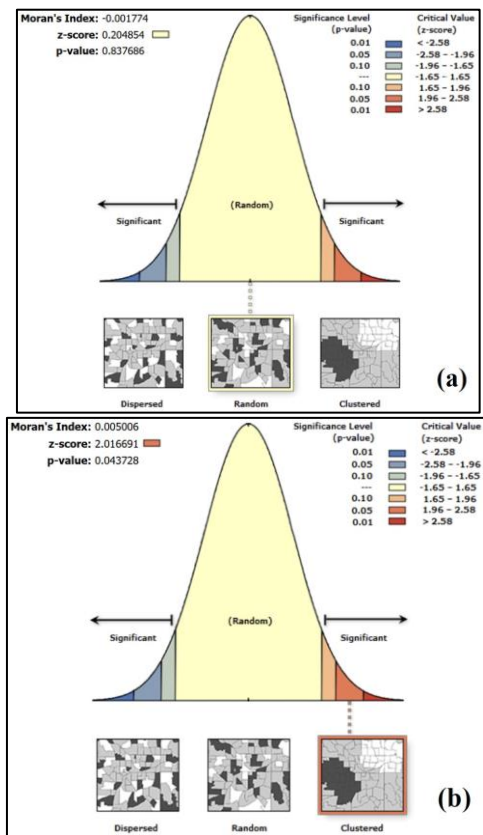


Fig. 7: Spatial autocorrelation using Moran's I index of the areas (sq.m) of (a) rubber tree less than 7 years old; (b) rubber tree between 7 and 15 years old; (c) rubber tree between 15 and 25 years old; (d) rubber tree greater than 25 years old

Conclusion

This study categorizes rubber tree stands into four growth stages based on their age: Less than 7 years old, 7-15 years old, 15-25 years old, and greater than 25 years old. The classification is done using OBIA techniques on Sentinel-2A imagery data. To begin, the specific rubber plantation area is mapped by visually interpreting high-resolution satellite imagery from Google Earth. This is done by digitizing the screen at a zoom scale of no more than 1:4,000.

The classification results indicate that the rubber plantation covers an area of 443.78 square kilometers, which represents 34.72% of the total area. In Step 2, rubber stand ages are classified using OBIA from Sentinel-2A imagery data. This involves defining 25 training areas for each rubber stand age, totaling 100 points.

Afterward, validate it by utilizing data collected from multiple field surveys. To determine the sample points for each age group based on the size of the area, a random stratified sampling method was employed. The breakdown of the sample points is as follows: 71 rubber trees are less than seven years old, 169 are between seven and fifteen

years old, 179 are between fifteen and twenty-five years old and 89 are older than twenty-five years. Then, an error matrix was generated and overall accuracy as well as the Kappa coefficient of agreement were calculated using information gathered from the field surveys.

The results showed that rubber in the age range of 7-15 years old had the largest area, covering 38.13% of the total area, which is equivalent to 169.23 square kilometers. This was followed by rubber in the age range of 15-25 years old, rubber less than 7 years old, and rubber older than 25 years old, occupying areas of 99.40 (22.40%), 96.85 (21.82%) and 78.30 (17.64%) square kilometers, respectively. The accuracy of the interpretation results corresponded to the spatial autocorrelation indices in the age range, with levels of -0.001774, 0.005006, 0.083034, and, 0.118706 respectively.

The distribution of areas within each age group was found to be mixed, mainly due to a lack of planning in planting zoning. Each farmer cultivates a different plant, with specific rubber stand ages for each age group. This information is crucial for assessing and planning future yields, especially for rubber timber that has reached felling maturity. In the next study, to improve the accuracy of rubber stand age classification using Object-Based Image Analysis (OBIA), the rubber age ranges should be correctly defined and high-resolution remote sensing data, such as the High-Resolution Imaging Satellite and unmanned aerial systems, should be combined.

Acknowledgment

This research project received financial support from Mahasarakham University through the Research Unit of Geo-informatics. The funding was specifically allocated for spatial management, spatial analysis, and the usage of the GIS laboratory.

Funding Information

This research project was financially supported by Mahasarakham University and Rubber Authority of Thailand (RAOT).

Author's Contributions

Jiradech Majandang: Conceptualization, tested, original drafted written, project administration.

Suepsai Prasansat: Conceptualization, methodology.

Patiwat Littidej: Conceptualization, tested, original draft writing, preparation, review and edited, supervision.

Phusit Khamphilung: Tested.

Nanthaporn Usaard: Methodology, preparation.

Benjamabhorn Pumhirunroj: Methodology.

Donald Slack: Review and edited.

Ethics

This is an original piece that has never been published before. The authors involved have reviewed and accepted this manuscript and have no ethical concerns related to this article. All respondents to this research were straightforward and responded in a simple manner. The purpose and stages of the study are provided. Consent was obtained from all respondents, ensuring that their participation was voluntary. Respondents have the freedom to decline participation. Furthermore, information about the respondents is treated discreetly and used solely for research purposes.

References

- Ahmad, A., & Quegan, S. (2014). Haze modelling and simulation in remote sensing satellite data. *Applied Mathematical Sciences*, 8(159), 7909–7921. <https://doi.org/10.12988/ams.2014.49761>
- Azizan, F. A., Kiloos, A. M., Astuti, I. S., & Abdul Aziz, A. (2021). Application of Optical Remote Sensing in Rubber Plantations: A Systematic Review. *Remote Sensing*, 13(3), 429. <https://doi.org/10.3390/rs13030429>
- Blagodatsky, S., Xu, J., & Cadisch, G. (2016). Carbon balance of rubber (*Hevea brasiliensis*) plantations: A review of uncertainties at plot, landscape and production level. *Agriculture, Ecosystems & Environment*, 221, 8–19. <https://doi.org/10.1016/j.agee.2016.01.025>
- Blaschke, T. (2010). Object based image analysis for remote sensing. *ISPRS Journal of Photogrammetry and Remote Sensing*, 65(1), 2–16. <https://doi.org/10.1016/j.isprsjprs.2009.06.004>
- Blaschke, T., Hay, G. J., Kelly, M., Lang, S., Hofmann, P., Addink, E., Queiroz Feitosa, R., van der Meer, F., van der Werff, H., van Coillie, F., & Tiede, D. (2014). Geographic Object-Based Image Analysis—Towards a new paradigm. *ISPRS Journal of Photogrammetry and Remote Sensing*, 87, 180–191. <https://doi.org/10.1016/j.isprsjprs.2013.09.014>
- Chen, B., Xiao, X., Wu, Z., Yun, T., Kou, W., Ye, H., Lin, Q., Doughty, R., Dong, J., Ma, J., Luo, W., Xie, G., & Cao, J. (2018a). Identifying Establishment Year and Pre-Conversion Land Cover of Rubber Plantations on Hainan Island, China Using Landsat Data during 1987–2015. *Remote Sensing*, 10(8), 1240. <https://doi.org/10.3390/rs10081240>
- Chen, G., Thill, J.-C., Anantsuksomsri, S., Tontisirin, N., & Tao, R. (2018b). Stand age estimation of rubber (*Hevea brasiliensis*) plantations using an integrated pixel- and object-based tree growth model and annual Landsat time series. *ISPRS Journal of Photogrammetry and Remote Sensing*, 144, 94–104. <https://doi.org/10.1016/j.isprsjprs.2018.07.003>

- Cleve, C., Kelly, M., Kearns, F. R., & Moritz, M. (2008). Classification of the wildland–urban interface: A comparison of pixel- and object-based classifications using high-resolution aerial photography. *Computers, Environment and Urban Systems*, 32(4), 317–326.
<https://doi.org/10.1016/j.compenvurbsys.2007.10.001>
- Center, C. (2023). *Loei Province Climate*. Thai Meteorological Department.
<http://climate.tmd.go.th/map/thailand>
- Congalton, R. G., & Green, K. (2008). *Assessing the Accuracy of Remotely Sensed Data* (2nd Ed.). CRC Press. <https://doi.org/10.1201/9781420055139>
- Dibs, H., & Hussain, T. H. (2018). Estimation and Mapping the Rubber Trees Growth Distribution using Multi Sensor Imagery with Remote Sensing and GIS Analysis. *Journal of University of Babylon, Pure and Applied Sciences*, 26(6), 109–123.
- Dibs, H., Idrees, M. O., & Alsalhin, G. B. A. (2017). Hierarchical classification approach for mapping rubber tree growth using per-pixel and object-oriented classifiers with SPOT-5 imagery. *The Egyptian Journal of Remote Sensing and Space Science*, 20(1), 21–30.
<https://doi.org/10.1016/j.ejrs.2017.01.004>
- Dong, J., Xiao, X., Chen, B., Torbick, N., Jin, C., Zhang, G., & Biradar, C. (2013). Mapping deciduous rubber plantations through integration of PALSAR and multi-temporal Landsat imagery. *Remote Sensing of Environment*, 134, 392–402.
<https://doi.org/10.1016/j.rse.2013.03.014>
- Drăguț, L., Tiede, D., & Levick, S. R. (2010). ESP: a tool to estimate scale parameter for multiresolution image segmentation of remotely sensed data. *International Journal of Geographical Information Science*, 24(6), 859–871.
<https://doi.org/10.1080/13658810903174803>
- FAOUN. (2022). *Crops and livestock products*. Food and Agriculture Organization of the United Nations. <https://www.fao.org/faostat/en/#data/QCL>
- Gibbes, C., Adhikari, S., Rostant, L., Southworth, J., & Qiu, Y. (2010). Application of Object Based Classification and High Resolution Satellite Imagery for Savanna Ecosystem Analysis. *Remote Sensing*, 2(12), 2748–2772.
<https://doi.org/10.3390/rs2122748>
- Hamada, Y., Stow, D. A., Roberts, D. A., Franklin, J., & Kyriakidis, P. C. (2013). Assessing and monitoring semi-arid shrublands using object-based image analysis and multiple endmember spectral mixture analysis. *Environmental Monitoring and Assessment*, 185(4), 3173–3190. <https://doi.org/10.1007/s10661-012-2781-z>
- Kajisa, T., Murakami, T., Mizoue, N., Top, N., & Yoshida, S. (2009). Object-based forest biomass estimation using Landsat ETM+ in Kampong Thom Province, Cambodia. *Journal of Forest Research*, 14(4), 203–211. <https://doi.org/10.1007/s10310-009-0125-9>
- Koedsin, W., & Huete, A. (2015). Mapping Rubber Tree Stand Age using Pléiades Satellite Imagery: A Case Study in Talang District, Phuket, Thailand. *Engineering Journal*, 19(4), 45–56.
<https://doi.org/10.4186/ej.2015.19.4.45>
- Kou, W., Xiao, X., Dong, J., Gan, S., Zhai, D., Zhang, G., Qin, Y., & Li, L. (2015). Mapping Deciduous Rubber Plantation Areas and Stand Ages with PALSAR and Landsat Images. *Remote Sensing*, 7(1), 1048–1073. <https://doi.org/10.3390/rs70101048>
- Lemes, E. M., Machado, T. V., Gontijo, L. N., de Andrade, S. L., Torres, J. L. R., Santos, M. A., & Coelho, L. (2020). Detection of rubber tree orchards infested by *Meloidogyne exigua* using vegetation indexes obtained from satellite images. *New Forests*, 51(5), 765–779. <https://doi.org/10.1007/s11056-019-09760-7>
- Li, Z., & Fox, J. M. (2012). Mapping rubber tree growth in mainland Southeast Asia using time-series MODIS 250 m NDVI and statistical data. *Applied Geography*, 32(2), 420–432.
<https://doi.org/10.1016/j.apgeog.2011.06.018>
- Lim, S. C., Gan, K. S., & Choo, K. T. (2003). The characteristics, properties and uses of plantation timbers-rubberwood and *Acacia mangium*. *Timber Technology Centre (TTC)*, 26, 1–11.
- Littidej, P., & Aunphoklang, W. (2013). Simulation of air pollution violence to potential area selection of the air quality monitoring station in Nakhon Ratchasima municipality, Thailand. *Pollution Research*, 32(2), 201–210.
- Littidej, P., Sarapirome, S., Aunphoklang, W., Tanang, S., Prasomsup, W. (2013). Frequency of violence mapping of air pollution using mathematical model and geographic information system. *34th Asian Conference on Remote Sensing, ACRS*, 5, 2207–2215.
- Littidej, P. (2017). Spatial Linear Programming Model to Reduce a Pollution Emissions of Sugarcane Transportation in Northeastern Thailand. *Pollution Research*, 36(2), 212–219.
<http://eprints.ukmc.ac.id/id/eprint/288>
- Littidej, P., Kromkratoke, W., Pumhirunroj, B., Buasri, N., Prasertsri, N., Sangpradid, S., Slack, D. (2024). Enhanced Rubber Yield Prediction in High-Density Plantation Areas Using a GIS and Machine Learning-Based Forest Classification and Regression Model. *Forests*, 15,1535.
<https://doi.org/10.3390/f15091535>

- Littidej, P., & Buasri, N. (2019). Built-Up Growth Impacts on Digital Elevation Model and Flood Risk Susceptibility Prediction in Muaeng District, Nakhon Ratchasima (Thailand). *Water*, 11(7), 1496. <https://doi.org/10.3390/w11071496>
- Littidej, P., Uttha, T., & Pumhirunroj, B. (2022). Spatial Predictive Modeling of the Burning of Sugarcane Plots in Northeast Thailand with Selection of Factor Sets Using a GWR Model and Machine Learning Based on an ANN-CA. *Symmetry*, 14(10), 1989. <https://doi.org/10.3390/sym14101989>
- Longseng, R., & Khaokong, C. (2020). Hexamethylene diamine-modified epoxidized natural rubber and its effect on cure characteristics and properties of natural rubber blends. *Iranian Polymer Journal*, 29(12), 1113–1121. <https://doi.org/10.1007/s13726-020-00865-x>
- Myint, S. W., Gober, P., Brazel, A., Grossman-Clarke, S., & Weng, Q. (2011). Per-pixel vs. object-based classification of urban land cover extraction using high spatial resolution imagery. *Remote Sensing of Environment*, 115(5), 1145–1161. <https://doi.org/10.1016/j.rse.2010.12.017>
- OAE. (2022). *Agricultural Statistics of Thailand 2021*. Ministry of Agriculture and Cooperatives. Office of Agricultural Economics. <https://oaezone.oae.go.th/view/22/Home/EN-US>
- Petsri, S., Chidthaisong, A., Pumijumng, N., & Wachrinrat, C. (2013). Greenhouse gas emissions and carbon stock changes in rubber tree plantations in Thailand from 1990 to 2004. *Journal of Cleaner Production*, 52, 61–70. <https://doi.org/10.1016/j.jclepro.2013.02.003>
- Phoomchai, T., Sangsing, K., Riyaphan, J., & Phoomchai, C. (2015). Chemical and Mechanical Properties in Hevea brasiliensis. *Thai Agricultural Research Journal*, 33(2), 144–158. <https://doi.org/10.14456/thaidoa-agres.2015.7>
- Prasertsri, N., & Littidej, P. (2020). Spatial Environmental Modeling for Wildfire Progression Accelerating Extent Analysis Using Geo-Informatics. *Polish Journal of Environmental Studies*, 29(5), 3249–3261. <https://doi.org/10.15244/pjoes/115175>
- Prasongsansuk, P., Thiangtrongjit, T., Nirapathpongorn, K., Viboonjun, U., Kongsawadworakul, P., Reamtong, O., & Narangajavana, J. (2020). Comparative proteomic analysis of differentially expressed proteins related to phloem and xylem development in rubber tree (Hevea brasiliensis). *Trees*, 34(6), 1467–1485. <https://doi.org/10.1007/s00468-020-02019-1>
- Pumhirunroj, B., Littidej, P., Boonmars, T., Artchayasawat, A., Prasertsri, N., Khamphilung, P., Sangpradid, S., Buasri, N., Uttha, T., & Slack, D. (2024). Spatial Predictive Modeling of Liver Fluke *Opisthorchis viverrine* (OV) Infection under the Mathematical Models in Hexagonal Symmetrical Shapes Using Machine Learning-Based Forest Classification Regression. *Symmetry*, 16, 1067. <https://doi.org/10.3390/sym16081067>
- Pumhirunroj, B., Littidej, P., Boonmars, T., Bootyothee, K., Artchayasawat, A., Khamphilung, P., & Slack, D. (2023). Machine-Learning-Based Forest Classification and Regression (FCR) for Spatial Prediction of Liver Fluke *Opisthorchis viverrini* (OV) Infection in Small Sub-Watersheds. *ISPRS International Journal of Geo-Information*, 12(12), 503. <https://doi.org/10.3390/ijgi12120503>
- Putklang, W., Mongkolsawat, C., & Suwanwerakamtorn, R. (2019). Object-based image analysis applied for different stages of rubber plantations mapping using THAICHOTE satellite data. *Journal of Theoretical and Applied Information Technology*, 97(6), 1720–1746.
- Rawat, J. S., & Kumar, M. (2015). Monitoring land use/cover change using remote sensing and GIS techniques: A case study of Hawalbagh block, district Almora, Uttarakhand, India. *The Egyptian Journal of Remote Sensing and Space Science*, 18(1), 77–84. <https://doi.org/10.1016/j.ejrs.2015.02.002>
- Rogan, J., Miller, J., Stow, D., Franklin, J., Levien, L., & Fischer, C. (2003). Land-Cover Change Monitoring with Classification Trees Using Landsat TM and Ancillary Data. *Photogrammetric Engineering & Remote Sensing*, 69(7), 793–804. <https://doi.org/10.14358/pers.69.7.793>
- Sarapirome, S., Aunphoklang, W., Littidej, P. (2013). Sugarcane transportation allocation using Multi-Objective Decision Analysis, Northeast region of Thailand. *34th Asian Conference on Remote Sensing, ACRS*, 5, 4128–4135.
- Sayavong, S., Kaewjampa, N., Katawatin, R., Iwai, C. B., Moukomla, S., Oszwald, J., & Pierret, A. (2019). Mapping rubber stand ages in Luangnamtha district (Northern Laos) usingNDVI and LSWIfrom Landsat images. *Asia-Pacific Journal of Science and Technology*, 24(2), 1–13. <https://doi.org/10.14456/apst.2019.18>
- Su, T., & Zhang, S. (2021). Object-based crop classification in Hetao plain using random forest. *Earth Science Informatics*, 14(1), 119–131. <https://doi.org/10.1007/s12145-020-00531-z>

- Suratman, M. N., Bull, G. Q., Leckie, D. G., Lemay, V. M., Marshall, P. L., & Mispan, M. R. (2004). Prediction models for estimating the area, volume, and age of rubber (*Hevea brasiliensis*) plantations in Malaysia using Landsat TM data. *International Forestry Review*, 6(1), 1–12.
<https://doi.org/10.1505/ifor.6.1.1.32055>
- Vu, V. T., Lai, V. L., Le, M. T., Huynh, D. D., Nguyen, T. T., Rivallan, R., Huynh, V. B., & Le Guen, V. (2020). Rubber tree accessions from wild Rondônia populations conserved in Vietnam. *Genetic Resources and Crop Evolution*, 67(2), 475–487.
<https://doi.org/10.1007/s10722-019-00843-0>
- Van Beilen, J. B., & Poirier, Y. (2007). Establishment of new crops for the production of natural rubber. *Trends in Biotechnology*, 25(11), 522–529.
<https://doi.org/10.1016/j.tibtech.2007.08.009>
- Yu, Q., Gong, P., Clinton, N., Biging, G., Kelly, M., & Schirokauer, D. (2006). Object-based Detailed Vegetation Classification with Airborne High Spatial Resolution Remote Sensing Imagery. *Photogrammetric Engineering & Remote Sensing*, 72(7), 799–811.
<https://doi.org/10.14358/pers.72.7.799>
- Yusof, N., Shafri, H. Z. M., & Shaharum, N. S. N. (2021). The use of Landsat-8 and Sentinel-2 imageries in detecting and mapping rubber trees. *Journal of Rubber Research*, 24(1), 121–135.
<https://doi.org/10.1007/s42464-020-00078-0>
- Zhang, C., & Xie, Z. (2013). Object-based Vegetation Mapping in the Kissimmee River Watershed Using HyMap Data and Machine Learning Techniques. *Wetlands*, 33(2), 233–244.
<https://doi.org/10.1007/s13157-012-0373-x>